SIMULTANEOUS MEASUREMENT OF ELECTRON BEAM SIZE AND DIVERGENCE WITH AN UNDULATOR *

B. X. Yang and A. H. Lumpkin
Advanced Photon Source, Argonne National Laboratory, Argonne, IL 60439, USA

Abstract

We present the simultaneous measurement of beam divergence and source size based on the APS diagnostic undulator line. A 300-μm-thick Si(400) crystal monochromator is used to measure the divergence with a resolution down to 3 μrad (1 μrad with the third harmonic). X-rays transmitted through the crystal are simultaneously used by a pinhole camera to measure the beam size, at a resolution of about 40 μm. We demonstrate that this measurement of emittance is robust against fluctuations of lattice functions due to a partial cancellation of systematic errors present in each of the measurements.

1 INTRODUCTION

Synchrotron radiation imaging is widely used for the measurement of beam size in electron/positron storage rings [1]. With knowledge of lattice beta functions, one can further deduce the particle beam emittance [1-4]. Similarly, undulator measurement of the beam divergence can also be used [3]. Since both of these approaches depend on accurate knowledge of the lattice functions, attempts have been made to use pinhole scan or multi-pinhole aperture measurement with undulator radiation to obtain the emittance independent of lattice functions [5,6]. To date these methods still require long time for data collection or analysis.

In this work, we present theory and an experiment for a new approach also based on undulator radiation. A thin-crystal monochromator is used to measure the x-ray beam divergence while a x-ray pinhole camera is used downstream of the crystal to measure the beam size at the same time. We will demonstrate that the combined measurement of emittance is robust against fluctuations of lattice functions due to a partial cancellation of systematic errors present in each of the measurements.

2 THEORETICAL BACKGROUND

The fully damped, stored electron beam can be well approximated by a Gaussian distribution in the 6-dimensional phase space involving two transverse coordinates (x, y) and angles (x', y'), time, and energy. For an undulator located in a dispersion-free region, we will take a simplified picture where only transverse components are considered in Eq. (1):

$$\rho(x,x',y,y') = \frac{\exp\left\{-\dfrac{\gamma_x x^2 + 2\alpha_x xx' + \beta_x x'^2}{2\varepsilon_x}\right\}}{2\pi\varepsilon_x} \cdot \{x \to y\}, \quad (1)$$

where α, β, γ are Twiss parameters and ε is the emittance. In this paper, we will use the center of the undulator as the origin of our coordinate system.

2.1 Monochromatic Divergence Measurement

A single electron traveling through the center plane of the undulator ($z=0$) with transverse coordinates (x, x', y, y') generates a radiation pattern on a downstream detector screen located at $z = S_m$. The pattern centers on the point $(x_m, y_m) = (x + S_m x', y + S_m y')$. For energies at or slightly above the nominal resonance of the undulator, the distribution function can be approximated by a Gaussian-like function [7] with its width given by $\sigma_m = \sqrt{\lambda / 2L}$, where L is the undulator length. Under this approximation, the two transverse dimensions are decoupled. Hence we will treat them separately. Multiplying the Gaussian response function with the distribution function of electrons in Eq. (1), and integrating over (x, x'), we get a Gaussian-shaped horizontal profile, with its width given by

$$S_m^2 \sigma_{x',eff}^2 = (S_m - Z)^2 \sigma_{x'}^2 + S_m^2 \sigma_m^2 + \sigma_{x0}^2 . \quad (2)$$

Here the location of the electron beam waist is $Z=\alpha/\gamma$, the width of the beam waist is σ_{x0}, and the beam divergence is $\sigma_{x'}$. For $S_m - Z_x >> \beta$, the divergence term dominates in this expression, while the beam size and undulator cone angle are just systematic errors to be corrected.

2.2 Pinhole Camera Source Size Measurement

If the monochromator crystal is thin, substantial high-energy x-ray flux will pass through it, enabling a pinhole camera to simultaneously record the source size. Again we will approximate the angular dependence of the photon beam with a Gaussian function (width σ_γ). For a pinhole located at a distance S from the undulator and S' from the detector screen, the geometrical optical approximation predicts that the image is a Gaussian function with a width, given in the source plane coordinates, of

$$\sigma_{x,eff}^2 = \frac{S^2\left(\sigma_{x'0}^2 + \sigma_\gamma^2 + \dfrac{Z^2}{\beta_0^2}\sigma_\gamma^2\right)}{\sigma_{x'0}^2 (S-Z)^2 + \sigma_\gamma^2 S^2 + \sigma_{x0}^2}\sigma_{x0}^2 . \quad (3)$$

* Work supported by U. S. Department of Energy, Office of Basic Energy Sciences under Contract No. W-31-109-ENG-38

For a long undulator ($\sigma_\gamma << \sigma_{x'}$) and a centered beam waist ($Z = 0$), Eq. (3) predicts that the measured effective size is smaller than the actual beam, due to the high collimation of the undulator beams. While the electrons' angular distribution is independent of their positions at the beam waist, the farther off-axis the electrons, the fewer photons they generate will pass through the pinhole. This results in a systematic error of a smaller measured effective source size, as pointed out previously [2,3,5]. This expression, based on simple geometrical optics models, applies only to the horizontal direction, where the beam size is much larger than the width of the camera point-spread-function (PSF).

2.3 Horizontal Beam Emittance

The expressions for effective divergence and beam size both show strong dependence on β functions, as well as the location of the beam waist, thus making them susceptible to magnetic lattice fluctuations. The product of these two numbers, however, is less dependent on them,

$$\varepsilon_{x,eff} = \sigma_{x,eff}\sigma_{x',eff} = \varepsilon\sqrt{\frac{\beta_0^2 + (S_m - Z)^2 + S_m^2\frac{\sigma_m^2}{\sigma_{x'}^2}}{\beta_0^2 + (S - Z)^2 + S^2\frac{\sigma_\gamma^2}{\sigma_{x'}^2}}\cdot\left(1+\frac{\beta\sigma_\gamma^2}{\beta_0\sigma_{x'}^2}\right)}, \quad (4)$$

where β_0 is the β function value at the beam waist.

(1) When the pinhole camera and the divergence measurement are using x-rays of the same energy, we may choose the location of monochromator and x-ray slits to be at the same distance from the undulator, $S_m = S$. Equation (4) can be further simplified to

$$\varepsilon \cong \sigma_{x,eff}\sigma_{x',eff}, \quad (5)$$

with a small correction term (less than 1% for the APS diagnostics undulator, $\sigma_\gamma \cong 2.6$ μrad and $\sigma_{x'} \cong 20$ μrad).

(2) When the pinhole camera is operating with a broad-band x-ray beam, σ_γ increases somewhat, but the correction to Eq. (5) is still expected to be small.

2.4 Fresnel Diffraction Broadening in y-Direction

The diffraction broadening of the pinhole image has been discussed by several authors [2,3], based on the hybrid model in which the geometric shadow of the pinhole and the Fraunhofer diffraction pattern were both approximated by Gaussian function, and the total broadening was assumed to be their convolution. Borland [5] appeared to be the first to point out the inadequacy of Fraunhofer diffraction and briefly discussed the effect of Fresnel diffraction. We have performed a detailed analysis of the PSF based on Fresnel diffraction. The PSF for monochromatic radiation for a pinhole aperture (width = *d*) can be written as the square of a Fresnel integral. It can be represented by an integral to allow analytical convolution with a Gaussian source function and a Gaussian spectrum function (polychromatic PSF). The result can then be compared directly with experimentally measured profiles.

3 EXPERIMENT

The experiment was performed at the diagnostics beam line of the Advanced Photon Source. The set up is shown in Figure 1 with relevant parameters given in Table 1.

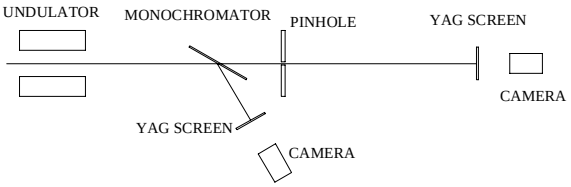

Figure 1: APS diagnostics undulator beamline

Table 1: Parameters for the APS undulator experiment

Undulator, period length, λ_u	18 mm
Undulator length, *L*	3.56 m
Undulator, fundamental photon energy	25.9 keV
Monochromator to undulator distance, S_m	27.47 m
Monochromator crystal	Si(400)
Monochromator crystal thickness	0.3 mm
Pinhole to undulator distance, *S*	28.56 m
Pinhole to x-ray camera distance, *S'*	9.13 m

3.1 Divergence Measurement

The Bragg reflection of a 300-μm Si(400) monochromator crystal was used for the divergence measurement. The crystal angle is chosen to be slightly lower than that for the resonance (10.13°). Integrated intensity profiles were obtained from digitized video images and fitted to Gaussian functions at video frequency (30 Hz). The data are logged at one-minute interval during user runs. Figure 2 shows such a log in a 12-hour run during December 1998. At high current in the fill, the horizontal beam size and divergence were high due to a subtle transverse instability [8]. As current decays, the divergences settle to values independent of the current,

$$\sigma_{x',eff} = 22.\varepsilon \pm 1\,(\mu\text{rad}), \text{ and } \sigma_{y',eff} = 3.2 \pm 0.2\,(\mu\text{rad}), \quad (7)$$

after correction for resolution (3 μrad).

3.2 Source Size from Pinhole Camera

The pinhole camera operates with a broad-band x-ray spectrum. The upstream 300-μm monochromator crystal at 10° grazing incidence angle is effectively a 1.73-mm thick silicon filter, which only allows photons above 15 keV to pass. The calculated angular distribution of the transmitted photons fits well to a Gaussian function (σ_γ=20.3 μrad). We also found that the measured horizontal intensity profile from the pinhole camera has

a nearly perfect Gaussian shape, giving an effective beam size $\sigma_{x,eff}$ = 360 (μm). Correction for instrument resolution is insignificant in this case.

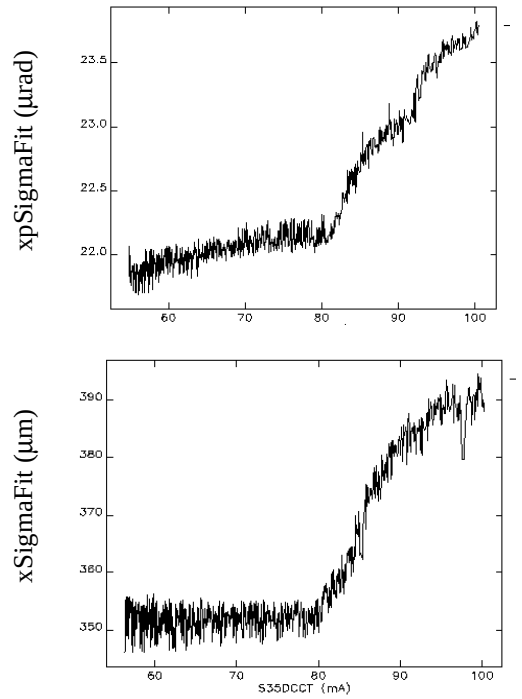

Figure 2: Beam data logged at 1-minute intervals. Upper panel: horizontal beam divergence (μrad); Lower panel: horizontal beam size (μm).

3.3 Horizontal Beam Emittance

Multiplying the effective beam divergence and size, we obtain the horizontal emittance ε_x = 7.9 ± 0.5 (nm rad). This agrees well with the measurement from the bending magnet sources.

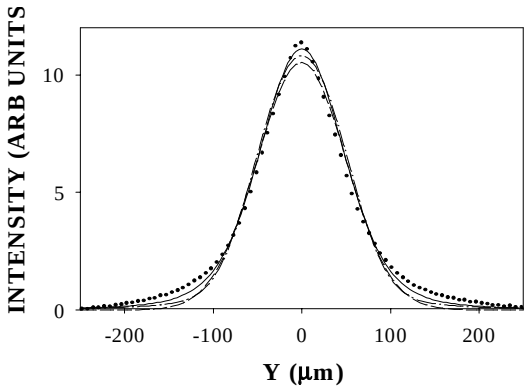

Figure 3: Integrated intensity profile in the vertical direction. (Dots) measured, (dashed line) Gaussian fit, (dash-dot) hybrid model fit with σ_x = 24 μm, and (solid line) Fresnel diffraction fit with σ_x = 34 μm.

3.4 Fresnel Diffraction in the Vertical Direction

Figure 3 shows the vertical intensity profile obtained from the pinhole image. Attempts to fit the profile with either a Gaussian function or a hybrid profile function failed due to the pronounced center peak and sidelobes. The polychromatic Fresnel model appears to improve the fit with an effective beam size of $\sigma_{y,eff}$ = 34 ± 7 (μm). The vertical emittance is thus ε_y = 0.11 (nm rad). This represents a vertical coupling of 1.4%, larger than that deduced from the measured beam size at the bending magnet source and measured beta functions.

4 SUMMARY

We reach the following conclusions from this work.

(1) By combining a thin monochromator crystal and a pinhole camera with a suitable undulator source, we have demonstrated experimentally that both electron beam divergence and size can be measured simultaneously. The current rate of measurement is limited by the speed of the camera/digitizer at about 30 Hz.

(2) While the lattice function and the properties of the undulator radiation can significantly affect either measured effective beam divergence or size, their product remains a good measure of emittance, robust against fluctuations of lattice α- and β-functions.

(3) We have presented experimental evidence showing that the Fresnel diffraction is valid and important in understanding x-ray pinhole camera data. Its introduction also pushes the fundamental resolution limit below that of the current, hybrid model by ~30%.

We wish to acknowledge G. Goeppner, I.-C. Sheng, E. Rotela, and S. Sharma for their help in beamline construction; M. Borland and L. Emery for help with the storage ring experiment; and G. Decker and J. Galayda for their continued support for the project.

5 REFERENCES

[1] A. Hofmann, "Beam Diagnostics and Applications," AIP Conf. Proc. **451** (3) 1998.

[2] P. Elleaume, C. Fortgang, C. Penel, E. Tarazona, "Measuring Beam Sizes and Ultra-Small Electron Emittances Using an X-Ray Pinhole Camera," J. Synch. Rad. **2**, (209) 1995.

[3] C. Zai et al., "Beam Size Measurement of the Stored Electron Beam at the APS Storage Ring Using Pinhole Optics," Rev. Sci. Instrum. **67**, (3368) 1996.

[4] B. X. Yang and A. H. Lumpkin, "Particle-Beam Profiling Techniques on the APS Storage Ring," AIP Proc. 390 (491) 1997.

[5] M. Borland, "A Method for Calculating emittance from Undulator Images," SSRL ACD-NOTES 60, 1989.

[6] C. Zai et al., "Phase-space Measurement of Stored Electron Beam at the Cornell Electron Storage Ring Using a Combination of Slit Array and CCD Detector," Rev. Sci. Instrum. **66**, (1859), 1995.

[7] K-J. Kim, "Characteristics of Synchrotron Radiation," AIP Conf. Proc. 184 (565) 1988.

[8] A. H. Lumpkin, L. Emery, and B. X. Yang, "Observations of 'Effective' Transverse Beam Size Instabilities for a High Current per Bunch Fill Pattern in the APS Storage Ring," these proceedings.